The Journal of Immunology

The AP-1 Transcription Factor c-Jun Promotes Arthritis by Regulating Cyclooxygenase-2 and Arginase-1 Expression in Macrophages

Nicole Hannemann, Jutta Jordan, Sushmita Paul, Stephen Reid, Hanns-Wolf Baenkler, Sophia Sonnewald, Tobias Bäuerle, Julio Vera, Georg Schett and Aline Bozec

J Immunol 2017; 198:3605-3614; Prepublished online 15 March 2017;
doi: 10.4049/jimmunol.1601330
http://www.jimmunol.org/content/198/9/3605

The Journal of Immunology is published twice each month by
The American Association of Immunologists, Inc.,
1451 Rockville Pike, Suite 650, Rockville, MD 20852

Print ISSN: 0022-1767 Online ISSN: 1550-6606.

The AP-1 Transcription Factor c-Jun Promotes Arthritis by Regulating Cyclooxygenase-2 and Arginase-1 Expression in Macrophages

Nicole Hannemann,* Jutta Jordan,† Sushmita Paul,‡ Stephen Reid,§ Hanns-Wolf Baenkler,* Sophia Sonnewald,§ Tobias Bäuerle,† Julio Vera,‡ Georg Schett,* and Aline Bozec*

Activation of proinflammatory macrophages is associated with the inflammatory state of rheumatoid arthritis. Their polarization and activation are controlled by transcription factors such as NF-κB and the AP-1 transcription factor member c-Fos. Surprisingly, little is known about the role of the AP-1 transcription factor c-Jun in macrophage activation. In this study, we show that mRNA and protein levels of c-Jun are increased in macrophages following pro- or anti-inflammatory stimulations. Gene Ontology and Kyoto Encyclopedia of Genes and Genomes pathway enrichment cluster analyses of microarray data using wild-type and c-Jun–deleted macrophages highlight the central function of c-Jun in macrophages, in particular for immune responses, IL production, and hypoxia pathways. Mice deficient for c-Jun in macrophages show an amelioration of inflammation and bone destruction in the serum-induced arthritis model. In vivo and in vitro gene profiling, together with chromatin immunoprecipitation analysis of macrophages, revealed direct activation of the proinflammatory factor cyclooxygenase-2 and indirect inhibition of the anti-inflammatory factor arginase-1 by c-Jun. Thus, c-Jun regulates the activation state of macrophages and promotes arthritis via differentially regulating cyclooxygenase-2 and arginase-1 levels. ***The Journal of Immunology*****, 2017, 198: 3605–3614.**

The transcription factor family AP-1 is composed of homo- and heterodimeric complexes, which consist of Jun, Fos, activating transcription factor, and musculoaponeurotic fibrosarcoma proteins. These dimers are involved in different cellular processes, such as proliferation, apoptosis, and differentiation (1). In macrophages, AP-1 proteins can regulate inflammatory processes through activation of cytokine production. For instance, the activation of IL and TLR leads to the initiation of an MAPK signaling cascade through MyD88, resulting in the activation of AP-1 in macrophages (2, 3).

Macrophages perform diverse homeostatic functions in the development, tissue repair, and immune responses against pathogens. Whereas resident macrophages regulate tissue homeostasis, macrophages recruited from the bloodstream activate specific transcriptional programs, which allow them to polarize into pro- or anti-inflammatory macrophages (4). AP-1 transcription factors have been described to orchestrate inflammatory responses in macrophages, in particular by the expression of inflammatory mediators (5). JunD for instance was recently shown to induce macrophage activation and cytokine secretion, by modulating their gene expression levels (6, 7). Furthermore, activation of JNK in macrophages is required for the establishment of obesity-induced insulin resistance and inflammation. JNK-deficient macrophages expressed fewer proinflammatory chemokines and cytokines, such as *Ccl2*, *Ccl5*, *IL-6*, *IL-12*, and *TNF* (8). Additionally, JNK blockade suppresses matrix metalloproteinases and thus inhibits arthritic joint destruction in a rat adjuvant-induced arthritis model (9). One JNK target is c-Jun, suggesting that c-Jun could also represent a potent regulator of macrophage activation during inflammation.

About 1% of the population worldwide is afflicted by rheumatoid arthritis, a chronic inflammatory disease of the joints, which is characterized by synovial hyperplasia, cartilage degradation, and bone destruction (10). Macrophages are centrally involved in the process of arthritis (11). Their numbers in the synovial membrane are increased during arthritis and exhibit a highly activated phenotype with increased expression of proinflammatory cytokines (12). In addition to their proinflammatory properties, they contribute to the destruction of bone and cartilage in the acute and chronic phases of arthritis (12). However, whether AP-1 proteins in macrophages influence inflammatory arthritis still remains unknown.

In this study, we show that c-Jun participates in macrophage activation by regulating the expression pattern of pro- and anti-inflammatory genes upon the stimulation with diverse Th1 or Th2 cytokines, pro- or anti-inflammatory stimulations, and microbial products. Gene Ontology (GO) cluster analysis unravels the important role of c-Jun in immune pathways and IL production. Two targets of c-Jun identified were the proinflammatory enzyme

*Department of Internal Medicine 3—Rheumatology and Immunology, University Hospital Erlangen, Friedrich Alexander University Erlangen–Nuremberg, 91054 Erlangen, Germany; †Preclinical Imaging Platform Erlangen, Institute of Radiology, University Hospital Erlangen, 91054 Erlangen, Germany; ‡Laboratory of Systems Tumor Immunology, Department of Dermatology, University Hospital Erlangen, 91054 Erlangen, Germany; and §Division of Biochemistry, Friedrich Alexander University Erlangen–Nuremberg, 91054 Erlangen, Germany

ORCIDs: 0000-0002-9185-6255 (S.S.); 0000-0002-3076-5122 (J.V.); 0000-0001-8174-2118 (A.B.).

Received for publication August 2, 2016. Accepted for publication February 17, 2017.

This work was supported by funding from the Staedtler Foundation, Deutsche Forschungsgemeinschaft Grants A01-CRC1181, Z-CRC1181, SPP1468 (IMMUNOBONE program), and BO3811/1-1 (Emmy Noether program), and by Interdisziplinäre Zentrum für Klinische Forschung Project D23.

The sequences presented in this article have been deposited in the National Center for Biotechnology Information's Gene Expression Omnibus database (https://www.ncbi.nlm.nih.gov/geo) under accession number GSE88898.

Address correspondence and reprint requests to Dr. Aline Bozec, Department of Internal Medicine 3—Rheumatology and Immunology, University Hospital Erlangen, Ulmenweg 18, 91054 Erlangen, Germany. E-mail address: aline.bozec@uk-erlangen.de

The online version of this article contains supplemental material.

Abbreviations used in this article: AC, apoptotic cell; Arg1, arginase-1; ChIP, chromatin immunoprecipitation; Cox2, cyclooxygenase-2; GO, Gene Ontology; KEGG, Kyoto Encyclopedia of Genes and Genomes; MRI, magnetic resonance imaging.

cyclooxygenase-2 (Cox2, also known as PG-endoperoxide synthase 2) and the anti-inflammatory enzyme arginase-1 (Arg1). Using two conditionally deleted c-Jun mice, controlled under the Mx-1 or the lysozyme 2 promoter, named c-Jun$^{\Delta Mx}$ or c-Jun$^{\Delta LysM}$, respectively, we confirmed the direct activation of Cox2 and the indirect inhibition of Arg1 by c-Jun. Moreover, using the K/BxN arthritis model, we showed reduced joint inflammation in c-Jun–deficient mice by histological analyses and in vivo magnetic resonance imaging (MRI). Finally, we confirmed the direct binding of c-Jun on the *Cox2* promoter in macrophages through chromatin immunoprecipitation (ChIP). Hence, c-Jun deletion in macrophages alters their activation state and ameliorates arthritis.

Materials and Methods

Animals

The generation of Jun$^{\Delta Mx}$ and c-Jun$^{\Delta LysM}$ mice was described elsewhere (13–15). The mice were bred and maintained on a 129/C57BL/6 background. Littermate mice were used as controls. All experiments were performed with male or female mice at the age of 12 wk. Animals were housed in standardized conditions following the guidelines of the German Animal Welfare Act. Animals were kept on a standard diet and water ad libitum and kept with a 12-h light/dark cycle. All animal experiments were authorized by the local ethics committee. The deletion of c-Jun by Mx1 promoter was induced by 250 μg of polyinosinic-polycytidylic acid (InvivoGen, San Diego, CA) injected i.p. three times every second day.

Thioglycollate-elicited peritoneal macrophages

Brewer's thioglycollate broth (4%; Sigma-Aldrich, Munich, Germany) was boiled, autoclaved, and aged for at least 1 mo prior to use. Mice were injected i.p. with 2.5 ml of 4% thioglycollate and sacrificed 72 h after. Peritoneal cells were harvested by peritoneal lavage with ice-cold PBS; cells were counted using a Neubauer chamber. Cells (1×10^6) were plated in RPMI 1640 (Life Technologies, Thermo Fisher Scientific) supplemented with 10% FCS (Life Technologies, Thermo Fisher Scientific) and 1% penicillin/streptomycin (Life Technologies, Thermo Fisher Scientific). Adherent cells were used the next day for stimulation with 50 ng/ml PMA (Sigma-Aldrich), 1 μg/ml LPS (Sigma-Aldrich), 50 ng/ml flagellin (InvivoGen), 50 ng/ml poly(deoxyadenylic-deoxythymidylic) acid (InvivoGen), 100 ng/ml IL-4 (Miltenyi Biotec, Bergisch Gladbach, Germany), 50 ng/ml IL-13 (Sigma-Aldrich), 50 ng/ml IFN-γ (PeproTech, Rocky Hill, NJ), 310 pg/ml TNF (Sigma-Aldrich), 1 ng/ml IL-6 (Sigma-Aldrich), 340 pg/ml IL-1β (Sigma-Aldrich), and 5×10^6 apoptotic cells (AC).

Generation of AC

To generate AC, splenocytes isolated from C57BL/6 mice were incubated in RPMI 1640 (Life Technologies, Thermo Fisher Scientific) supplemented with 10% FCS (Life Technologies, Thermo Fisher Scientific) and 1% penicillin/streptomycin (Life Technologies, Thermo Fisher Scientific) and in the presence of 1 μM dexamethasone (Sigma-Aldrich). After 12 h, the splenocytes were washed several times with PBS, spun through an FCS cushion to eliminate the dexamethasone, and resuspended in complete medium again. AC were checked by annexin V/propidium iodide staining and the macrophages were incubated with AC (1:5 ratio) at 37°C for the indicated times.

RNA isolation, reverse transcription, and real-time PCR

Total RNA of paws was isolated with peqGOLD TriFast and total RNA of cells was isolated with TriFast (Peqlab–Life Science/VWR International, Radnor, PA) according to the manufacturer's instruction. One microgram of total RNA was digested with 1 U DNase I (Invitrogen, Life Technologies) according to the manufacturer's instructions and subsequently used to synthesize cDNA with reagents from a high-capacity cDNA reverse transcription kit (Applied Biosystems, Life Technologies). The quantitative PCR reactions were performed using SYBR select master mix (Applied Biosystems, Life Technologies). The $2^{-\Delta\Delta Ct}$ method was used to quantify amplified fragments, and *β-actin* as a housekeeping gene was used for normalization.

ChIP

ChIP was performed as described previously (16). *Cox2* and *Arg1* promoter regions were amplified with specific primers for the corresponding promoter sites by real-time PCR. The percentage binding of input was determined as $(2^{Ct\ input\ -\ Ct\ sample}) \times 100$.

Western blot analysis

Cells were lysed using Frackelton buffer (10 mM Tris, 50 mM NaCl, 30 mM NaPPi, 50 mM NaF, 1% Triton X-100) supplemented with protease inhibitor mixture (cOmplete ULTRA; Roche, Basel) followed by three freeze and thaw cycles in liquid nitrogen. Afterward, lysates were boiled for 5 min in 1× Laemmli buffer and centrifuged. Cell extracts from 0.25×10^6 macrophages were separated by $NaDodSO_4$-PAGE on a 10% acrylamide gel. Semidry immunoblotting was carried out on polyvinylidene difluoride membrane, which was further incubated overnight at 4°C with rabbit anti-mouse c-Jun (1:1000; Cell Signaling Technology, Leiden, the Netherlands), rabbit anti-mouse GAPDH (1:5000; Cell Signaling Technology), and mouse anti-mouse β-actin Ab (1:5000; Sigma-Aldrich, St. Louis, MO) and the respective secondary Ab, rabbit IgG or mouse IgG conjugated with HRP (Promega, Madison, WI).

PGE_2 enzyme immunoassay

PGE_2 was measured in whole-paw lysates using an enzyme immunoassay kit–monoclonal (Cayman Chemical, Ann Arbor, MI), according to the manufacturer's instructions.

Arginase activity assay

Arginase assays were performed with whole-paw lysates as described previously (17).

Microarray gene expression profiling

Total RNA was isolated from 1×10^6 peritoneal macrophages from c-Jun$^{\Delta LysM}$ or wild-type littermates, respectively, with an RNeasy mini kit (Qiagen, Hilden, Germany). cRNA was synthesized with Cy3 labeling, quantified, and hybridized on 8 × 60K arrays (design ID 028005; Agilent Technologies, Santa Clara CA). Data were extracted by the Feature Extraction software package (v11.7.1; Agilent Technologies) using a standard protocol. Text files generated by the Feature Extraction software were imported into GeneSpring GX v12.5 (Silicon Genetics, Palo Alto, CA). Data were $\log_2$ transformed followed by normalization to the 75th percentile and corrected to the median of all samples. Features passing the quality check (flags detected in at least one condition) and showing changes in expression levels ≥2-fold were selected for further analysis. A volcano plot was applied to identify statistically significant ($p > 0.05$), >2-fold differentially expressed genes between two conditions including the Benjamini–Hochberg multiple test correction. The data are deposited in National Center for Biotechnology Information's Gene Expression Omnibus (https://www.ncbi.nlm.nih.gov/geo/query/acc.cgi?acc=GSE88898).

Coregulation networks and comparative bioinformatics

For the biological interpretation of selected differentially expressed genes, the Cytoscape (18) plugin ClueGO (19) was used. It visualizes the non-redundant biological terms for large clusters of genes in a functionally grouped network. The related terms that share similar associated genes can be fused to reduce redundancy; those terms have the same color code. The ClueGO network is created with κ statistics and reflects the relationships between the terms based on the similarity of their associated genes. In the network, the node color can be switched between functional groups and cluster distributions. The association of genes with a term is calculated in terms of p value. For correction of a p value, the Bonferroni step-down method was used. The lower the p value, the more significant is the term. The size of the nodes in the network represents the statistical significance level of that term. The largest node in the cluster denotes that the term is the most significant one and that it is also the representative term of the cluster. For the current analysis, the threshold for statistical significance was set to $p = 0.05$ and the minimum number of genes associated with a term was set to three. The ClueGO plugin was used to do both GO enrichment analysis as well as to do pathway enrichment analysis using Kyoto Encyclopedia of Genes and Genomes (KEGG) databases.

KRN TCR-transgenic mouse serum–induced arthritis model

KRN TCR-transgenic mice were bred to NOD/Lt mice to generate K/BxN mice (20). K/BxN serum pools were prepared from adult arthritic mice. Arthritis was induced by i.p. injection of 150 μl of K/BxN serum. Arthritis was monitored by measuring the thickness of both hind paws using a dial caliper. The arthritis score was determined as described elsewhere (21).

Histological analysis

Mouse paws were dissected, fixed in 4% formalin, and decalcified in 14% (w/v) EDTA until the bone became fragile. The paws were paraffin

embedded and cut into 2-μm sections. The sections were stained for tartrate-resistant acid phosphatase using a leukocyte acid phosphatase kit (Sigma-Aldrich) according to the manufacturer's instructions or with H&E. The analyses were performed using a microscope (Nikon) and an image analysis system for performing histomorphometry (OsteoMeasure; OsteoMetrics, Decatur, GA).

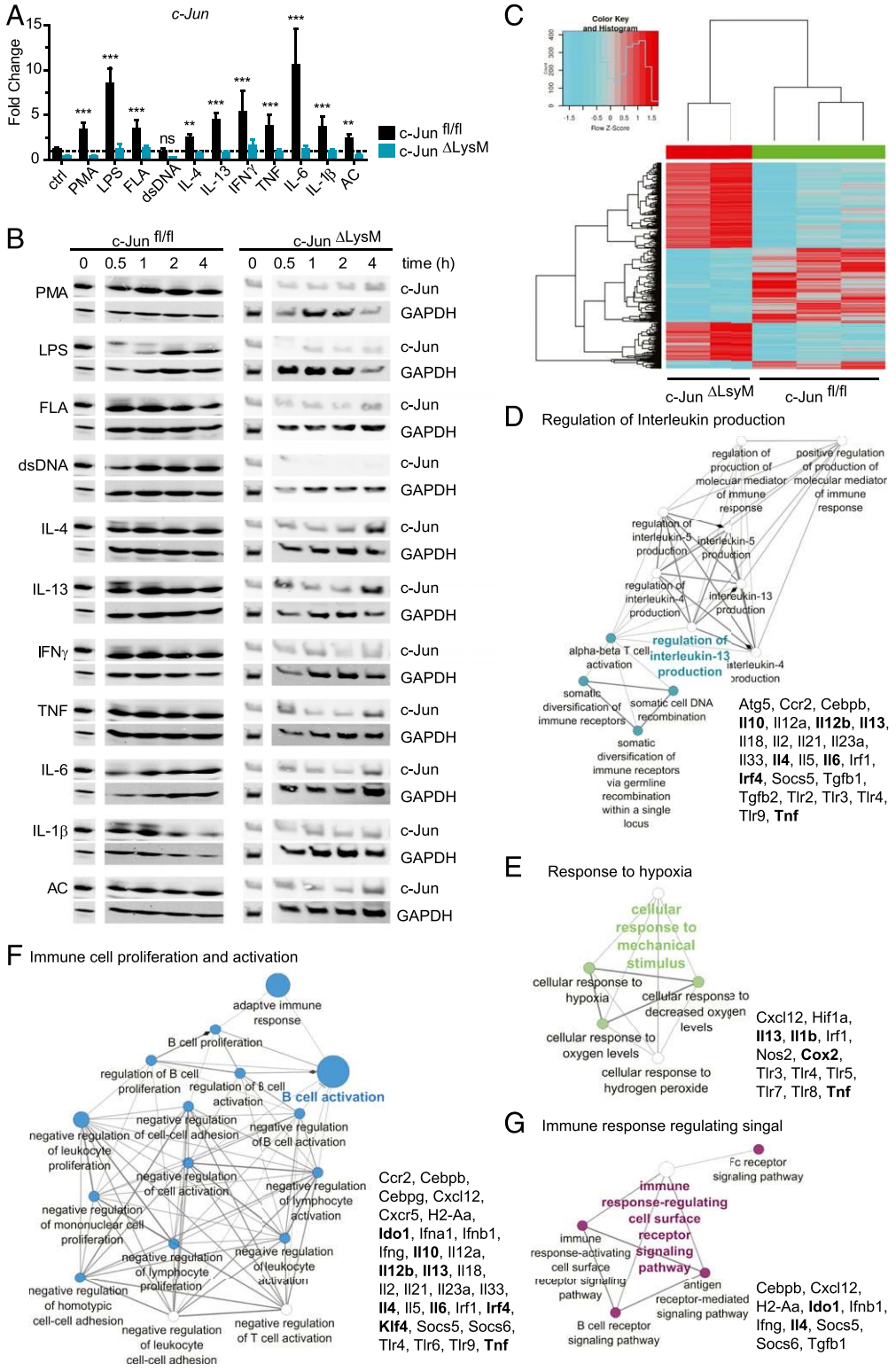

FIGURE 1. Genome-wide analyses of c-Jun network in macrophages. (**A** and **B**) Thioglycollate-elicited macrophages (1×10^6) from c-Jun$^{\Delta LysM}$ or control mice were stimulated with 50 ng/ml PMA, 1 μg/ml LPS, 50 ng/ml flagellin (FLA), 50 ng/ml dsDNA, 100 ng/ml IL-4, 50 ng/ml IL-13, 50 ng/ml IFN-γ, 310 pg/ml TNF, 1 ng/ml IL-6, 340 pg/ml IL-1β, and 5×10^6 AC. (A) Quantitative real-time PCR of *c-Jun* mRNA levels were determined 30 min after stimulations. Data are shown as means of three independent experiments, and the error bars represent SEM. $^{**}p < 0.01$, $^{***}p < 0.001$ by Student *t* test. (B) c-Jun protein levels were determined by Western blotting at the indicated time points after stimulations. The same c-Jun and GAPDH blots from time 0 (unstimulated macrophage) were taken as reference for all the stimulations. (**C**) Heat map of differentially expressed genes ascertained from microarray analysis of mRNA isolated from peritoneal macrophages of c-Jun$^{\Delta LysM}$ ($n = 2$) or littermate controls ($n = 3$). (**D**–**G**) GO cluster analysis (cutout from Supplemental Fig. 2) based on the differentially expressed genes found in the microarray analysis.

Flow cytometry

For flow cytometry analysis of the paw, single-cell suspensions were prepared by mincing the tissue and subsequent collagenase A (Biochrom, Merck Millipore, Berlin, Germany) digestion for 60 min at 37°C. For cell surface staining the cell suspension was blocked with 0.5 μg/ml anti-mouse CD16/32 (BioLegend, San Diego, CA) for 10 min at 4°C and subsequently incubated with directly conjugated Abs: 0.5 μg/ml anti-mouse CD45–eFluor 780 (eBioscience, San Diego, CA), 0.5 μg/ml anti-mouse F4/80-PE (BioLegend), 0.5 μg/ml anti-mouse CD11b-PE-Cy7 (eBioscience), and 0.6 μg/ml anti-mouse I-A/I-E–Pacific Blue (BioLegend). For intracellular staining of Cox2, an intracellular fixation and permeabilization buffer set (eBioscience) was used, blocked with PBS containing 2% rabbit serum/0.1% BSA and 0.5 μg/ml anti-mouse CD16/32 (BioLegend), and subsequently stained with the following Abs: 1.6 μg/ml goat anti-mouse Cox2 (Abcam, Cambridge, MA) or 1.6 μg/ml goat IgG isotype (Abcam), 0.5 μg/ml rabbit anti-goat IgG-biotin (Abcam), and streptavidin-FITC (SouthernBiotech, Birmingham, AL).

Magnetic resonance imaging

For determination of soft tissue paw volume ex vivo, excised hind legs were processed in 4% agarose and placed in a small animal ultra–high-field magnetic resonance scanner (ClinScan 7 Tesla; Bruker, Ettlingen, Germany). A standard T1-weighted gradient echo sequence was used for segmentation of the soft tissue volume by dedicated software (aycan OsiriX with a plugin; aycan Digitalsysteme, Würzburg, Germany and Chimaera, Erlangen, Germany).

For in vivo MRI, mice under inhalation anesthesia were imaged using the whole-body mouse coil in the ultra–high-field magnetic resonance scanner (ClinScan 7 Tesla; Bruker). A standard T1-weighted spin echo sequence was used for segmentation of the paw volume. Furthermore, dynamic contrast-enhanced MRI was performed by a three-dimensional flash sequence before, during, and after i.v. contrast agent application (0.2 mmol/kg, Gadavist; Bayer, Leverkusen, Germany). For postprocessing of imaging data, a region of interest was placed in the foot to determine dynamic contrast-enhanced MRI parameters of vascularization on signal intensity–versus–time curves, that is, area under the curve, peak enhancement, and time to peak using the above-mentioned software (aycan OsiriX; aycan Digitalsysteme).

Statistical analysis

All experiments were repeated at least three times. Statistical analysis was performed using GraphPad Prism software (version 5.03). Prior to statistical analysis, Gaussian distribution of the values was tested; when the values passed the normality test, a Student *t* test was used for comparison of two groups. For not normally distributed values, a Mann–Whitney *U* test was used. For multiple comparisons, a two-way ANOVA with a Bonferroni posttest was used. A p value <0.05 was considered significant. Data are shown as means, and the error bars represent SEM.

Results

Increased expression of c-Jun following macrophage stimulations

To determine the importance of c-Jun during macrophage activation, we analyzed the expression of c-Jun at mRNA and protein levels in thioglycollate-elicited macrophages following various

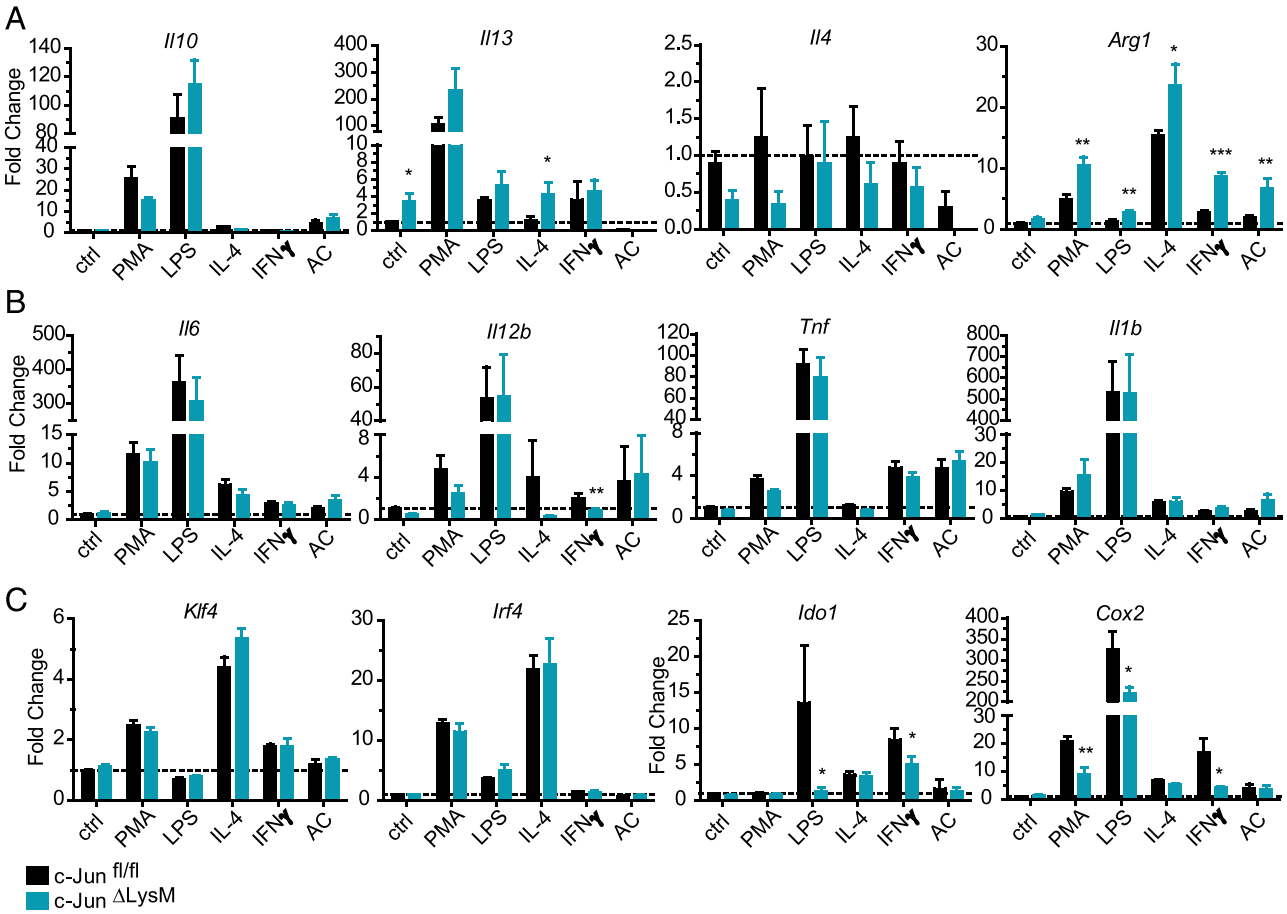

FIGURE 2. Differentially expressed genes in c-Jun–deleted macrophage mice following pro- and anti-inflammatory stimulations. Thioglycollate-elicited macrophages (1×10^6) from c-Jun$^{\Delta LysM}$ or littermate control mice were stimulated with 50 ng/ml PMA, 1 μg/ml LPS, 100 ng/ml IL-4, 50 ng/ml IFN-γ, or 5×10^6 AC. The mRNA levels of (**A**) anti-inflammatory molecules (*Il10*, *Il13*, *Il4*, and *Arg1*), (**B**) proinflammatory molecules (*Il6*, *Il12b*, *Tnf*, and *Il1b*), and (**C**) signaling molecules (*Klf4*, *Irf4*, *Ido1*, and *Cox2*) were determined 2 h after stimulations by quantitative real-time PCR. Data are shown as means of three independent experiments, and the error bars represent SEM. $*p < 0.05$, $**p < 0.01$, $***p < 0.001$ by Student *t* test.

stimulations. Quantitative analyses of *c-Jun* mRNA levels in macrophages revealed an increased *c-Jun* expression 30 min after stimulation with AC, PMA, the Th1 cytokines IFN-γ and TNF, and the Th2 cytokines IL-4 and IL-13, but also microbial products such as LPS and flagellin (Fig. 1A, Supplemental Fig. 1A). However, dsDNA did not induce *c-Jun* expression in macrophages (Fig. 1A). In accordance, protein analysis revealed increased c-Jun protein and c-Jun phosphorylation already 30 min after stimulation (Fig. 1B, Supplemental Fig. 1B), suggesting an active role of c-Jun during macrophage signaling.

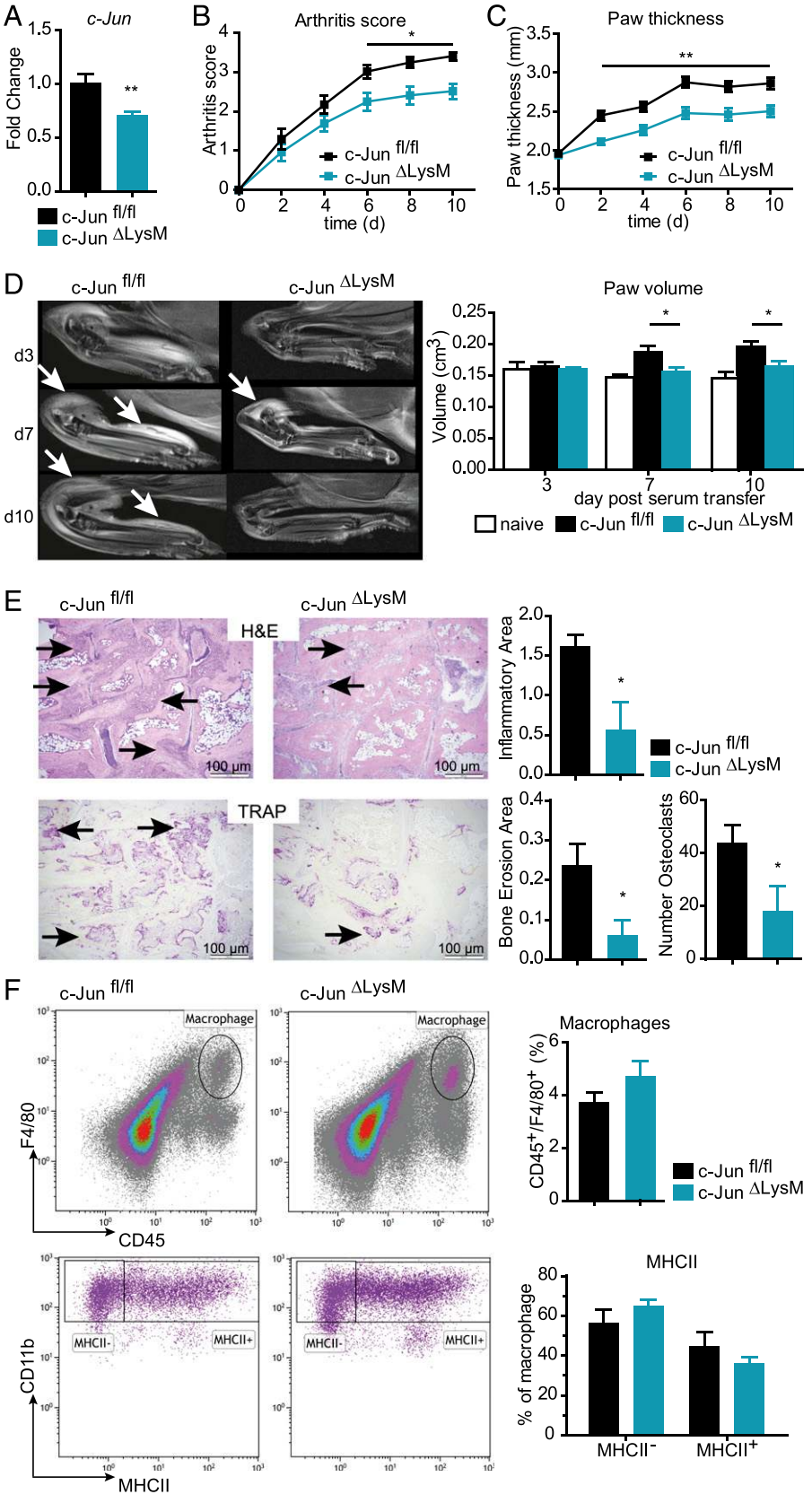

FIGURE 3. Alleviated arthritis in c-Jun$^{\Delta LysM}$ mice. Arthritis was induced by K/BxN serum transfer in c-Jun$^{\Delta LysM}$ or wild-type littermate mice. (**A**) *c-Jun* mRNA levels in whole paws were measured at day 10 after serum transfer by quantitative real-time PCR (n = 10). (**B**) The arthritis score was evaluated and (**C**) the paw thickness was determined at the indicated time points (n = 7). (**D**) Representative images of in vivo MRI analysis of healthy controls (naive) as well as wild-type and c-Jun$^{\Delta LysM}$ paws at days 3, 7, and 10 after serum transfer and the corresponding quantification of the paw volume (n = 6). (**E**) Histological analysis of H&E and tartrate-resistant acid phosphatase (TRAP) staining was performed at day 10 after serum transfer and the respective quantification of the inflammatory area, erosion area, and number of osteoclasts (n = 6). (**F**) The cell populations were quantified by flow cytometry at day 10 after serum transfer in the paws. Macrophages were defined as CD45$^+$ and F4/80$^+$ cells, and the presence of MHC class II was used to determine their subpopulations. Shown are representative dot plots and the quantification of the gating in percentage. Data are shown as means, and the error bars represent SEM. *$p < 0.05$, **$p < 0.01$ by Student t test (A, E, and F), Mann–Whitney U test (B and C), or ANOVA (D).

Table I. Macrophage numbers in paws of arthritic mice

	c-Jun$^{fl/fl}$	c-Jun$^{\Delta LysM}$
Macrophages	15,883 ± 2,798	15,392 ± 2,974
MHC$^-$	8,862 ± 1,561	9,344 ± 1,805
MHC$^+$	7,021 ± 1,237	6,041 ± 1,167

The cell populations were quantified by FACS at day 10 after serum transfer in the paws of wild-type and c-Jun$^{\Delta LysM}$ mice. Macrophages were defined as CD45$^+$ and F4/80$^+$ cells, and the presence of MHC class II was used to determine their pro- and anti-inflammatory potential. Data are shown as mean values of absolute cell numbers per paw ± SD (n = 10).

Distinct transcriptional programs in c-Jun–deleted macrophages

To analyze the role of c-Jun in macrophages, we generated c-Jun conditional knockout mice using either lysozyme 2 (c-Jun$^{\Delta LysM}$) or Mx1 (c-Jun$^{\Delta Mx}$) promoters driving deletion. The analyses of thioglycollate-elicited macrophages isolated from c-Jun$^{\Delta LysM}$ or c-Jun$^{\Delta Mx}$ mice confirmed the deletion of *c-Jun* at the mRNA and protein levels (Fig. 1A, 1B, Supplemental Fig. 1). To determine the full profile of the c-Jun network, microarray RNA expression analysis using the Agilent Technologies platform was performed in wild-type and c-Jun$^{\Delta LysM}$ macrophages. More than 700 genes were detected to be differentially expressed when comparing peritoneal macrophages isolated from wild-type and c-Jun$^{\Delta LysM}$ mice (Fig. 1C). KEGG pathway enrichment and cluster analyses linked the differentially expressed transcripts to various signaling pathways important in autoimmune diseases, such as type 1 diabetes mellitus, inflammatory bowel disease, or rheumatoid arthritis (Supplemental Fig. 2A). Additionally, GO enrichment and cluster analysis revealed several pro- and anti-inflammatory gene-associated networks, such as immune cell proliferation, regulation of IL production, immune response signaling, and response to hypoxia (Fig. 1D–G, Supplemental Fig. 2B). Taken together, these data reveal that c-Jun is a central transcription factor during macrophage activation.

Decreased expression of Cox2 and increased expression of Arg1 in c-Jun–deleted macrophages

Based on microarray expression data, genes found altered in c-Jun–deleted unstimulated macrophages (Fig. 1D–G) were also tested at mRNA levels after macrophage stimulation in wild-type and c-Jun–deficient thioglycollate-elicited macrophages. As shown in Fig. 2, *Il13*, *Arg1*, *Il12b*, *Ido1*, and *Cox2* were found differentially expressed following distinct stimulations (Fig. 2). Other pro- and anti-inflammatory cytokines, such as *Il10*, *Il4*, *Il6*, *Tnf*, and *Il1b*, or signaling molecules, such as *Klf4* and *Irf4* mRNA levels, were not changed in c-Jun–deficient macrophages, as compared with wild-type macrophages (Fig. 2). Interestingly, the mRNA levels of the proinflammatory gene *Cox2* was significantly decreased in c-Jun–deleted macrophages at 2 h after PMA, LPS, or IFN-γ stimulations (Fig. 2C). However, the expression level of the anti-inflammatory gene *Arg1* was significantly increased 2 h after stimulation in c-Jun–deleted macrophages compared with wild-type macrophages (Fig. 2A). These data suggest that c-Jun might regulate the inflammatory state of macrophages by controlling *Cox2*, *Ido1*, and *Arg1* expression.

Two different genetic approaches of c-Jun deletion in macrophages show amelioration of arthritis

Next, we determined whether *c-Jun* expression in macrophages is of pathophysiological relevance. As suggested by the KEGG clustered microarray results (Supplemental Fig. 2A), inflammatory diseases such as rheumatoid arthritis could be a suitable readout to address this question. Indeed, *c-Jun* expression was significantly increased in arthritic mice joints as compared with nonarthritic mice (Supplemental Fig. 3A). Then, we induced serum-induced arthritis by K/BxN serum transfer in c-Jun$^{\Delta Mx}$ or c-Jun$^{\Delta LysM}$ mice and their respective littermate controls. First, *c-Jun* expression was determined after serum-induced arthritis induction in the joints of wild-type and c-Jun–deficient mice. The c-Jun deletion controlled by the Mx1 promoter leads to ∼50%

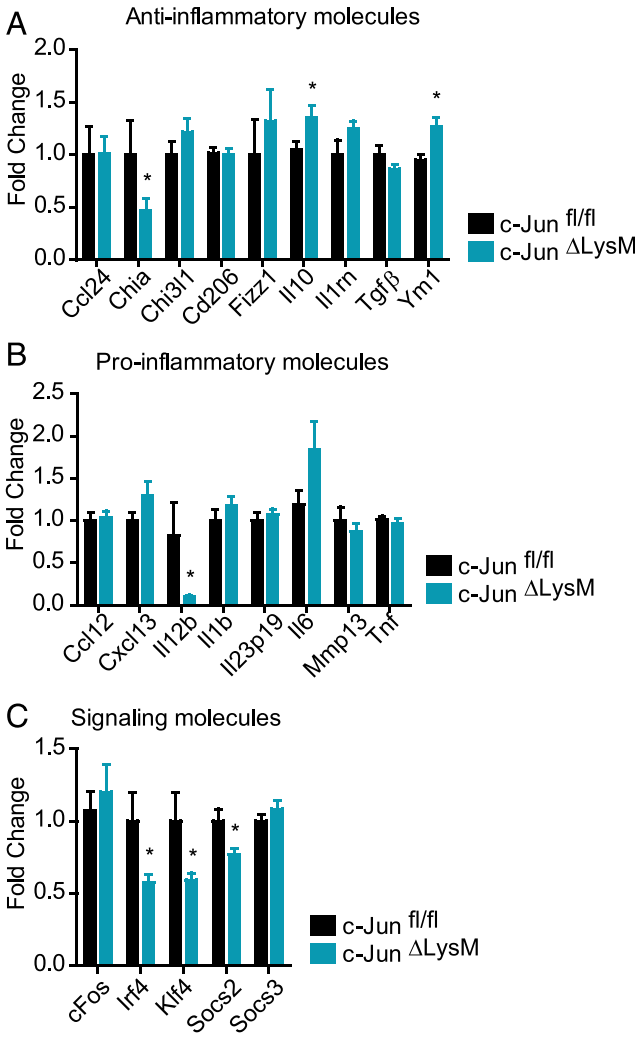

FIGURE 4. Differentially expressed genes in arthritic paws from c-Jun$^{\Delta LysM}$ mice compared with control mice. Arthritis was induced by K/BxN serum transfer in c-Jun$^{\Delta LysM}$ or littermate mice (n = 10). The mRNA from whole paws was isolated at day 10 after serum transfer, and the expression levels were determined by quantitative real-time PCR. (**A**) Anti-inflammatory molecules: *Ccl24*, *Chia*, *Chi3l1*, *Cd206*, *Fizz1*, *Il10*, *Il1rn*, *Tgfβ*, and *Ym1*. (**B**) Proinflammatory molecules: *Ccl12*, *Cxcl13*, *Il12b*, *Il1b*, *Il23p19*, *Il6*, *Mmp13*, and *Tnf*. (**C**) Signaling molecules: *cFos*, *Irf4*, *Klf4*, *Socs2*, and *Socs3*. Data are shown as means of three independent experiments, and the error bars represent SEM. *$p < 0.05$ by Student t test.

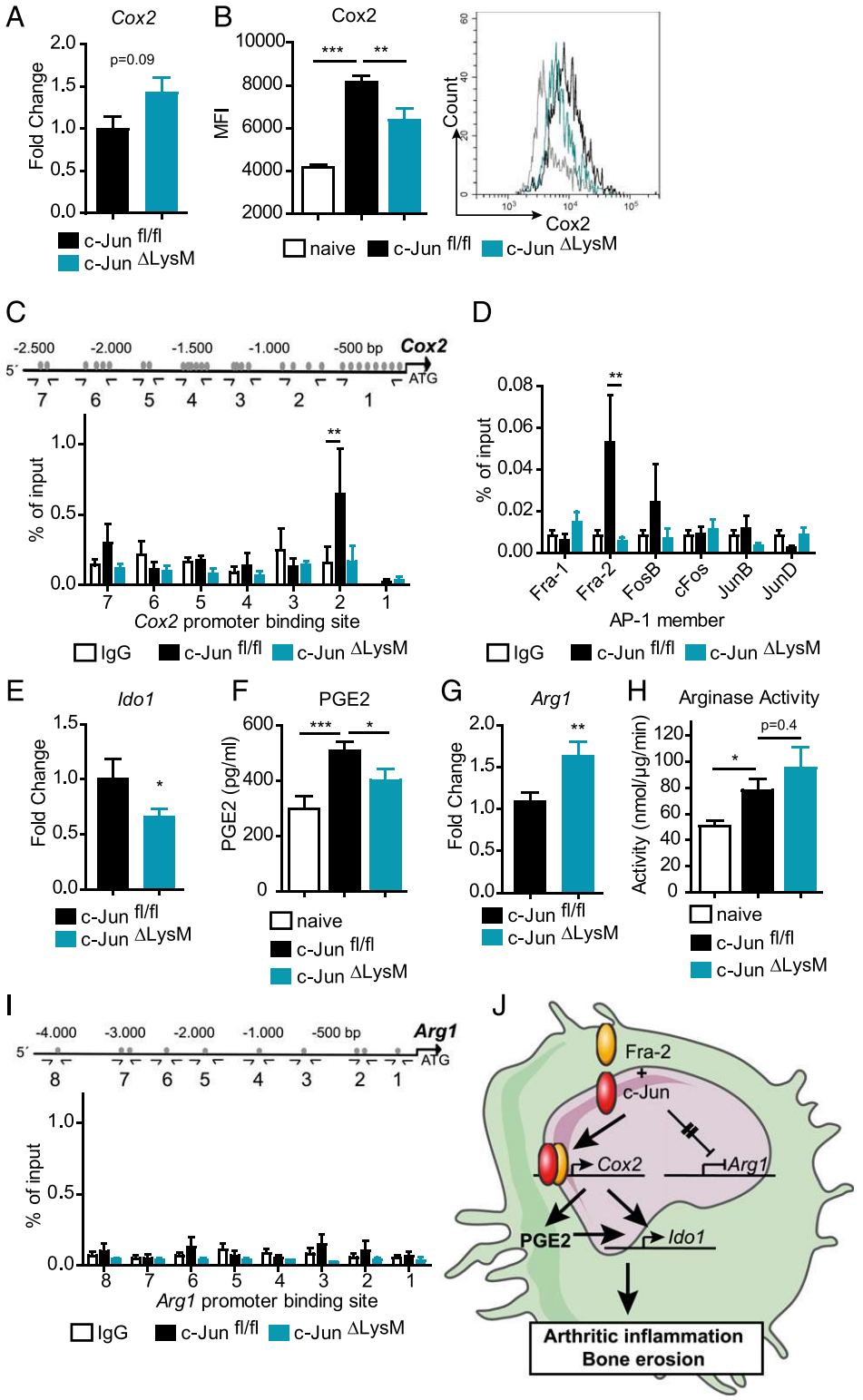

FIGURE 5. c-Jun induces Cox2 and inhibits Arg1 in macrophages. (**A** and **B**) Arthritis was induced by K/BxN serum transfer in c-Jun$^{\Delta LysM}$ and littermate mice; the analysis occurred 10 d after serum transfer. (A) *Cox2* mRNA level in joints was determined by real-time PCR (n = 10). (B) Cox2 protein levels in macrophages isolated from arthritic joints were determined by intracellular flow cytometry staining and are indicated as mean fluorescence intensity (MFI) (n = 6). (**C**) Model of the putative AP-1 binding sites at the promoter of *Cox2* and ChIP analysis of thioglycollate-elicited macrophages from c-Jun$^{\Delta LysM}$ or control mice; chromatin was precipitated using anti-mouse c-Jun or IgG isotype, and the eluate was quantified by real-time PCR with primers specific for the putative binding sites as indicated in the promoter scheme. The Ct values are normalized to the input. (**D**) ChIP analysis of thioglycollate-elicited macrophages from c-Jun$^{\Delta LysM}$ or control mice; chromatin was precipitated using anti-mouse Fra-1, Fra-2, FosB, cFos, JunB, JunD, or IgG-isotype; the eluate was quantified by real-time PCR with primers specific for the putative binding sites as indicated in the promoter scheme. The Ct values are normalized to the input. (**E**) *Ido1* mRNA level in joints of c-Jun$^{\Delta LysM}$ and their littermate mice (n = 10) by real-time PCR 10 d after serum transfer. (**F**) PGE_2 protein level in whole-paw lysates from c-Jun$^{\Delta LysM}$ mice and littermate controls 10 d after serum transfer (n = 8). (**G**) *Arg1* mRNA level in c-Jun$^{\Delta LysM}$ and control mice joints by real-time PCR 10 d after serum transfer (n = 10). (**H**) Arginase activity in whole-paw lysates from c-Jun$^{\Delta LysM}$ and control littermates mice 10 d postserum transfer (n = 6). (**I**) Model of the putative AP-1 binding sites at the promoter of *Arg1* and ChIP analysis of (*Figure legend continues*)

decreased *c-Jun* mRNA levels in paws from arthritic mice (Supplemental Fig. 3B). Interestingly, c-Jun$^{\Delta Mx}$ mice had reduced arthritis scores and paw swelling when compared with littermate controls (Supplemental Fig. 3C, 3D). Additionally, MRI analyses of the paws showed a reduced soft tissue volume in c-Jun$^{\Delta Mx}$ mice 10 d after induction of arthritis (Supplemental Fig. 3E). In accordance, the histological analysis of the mice paws revealed reduced cell infiltration in c-Jun$^{\Delta Mx}$ mice (Supplemental Fig. 3F). Additionally, the number of osteoclasts was reduced and the amount of arthritic bone erosion was decreased in c-Jun$^{\Delta Mx}$ mice, indicating a proinflammatory role of c-Jun during arthritis either due to regulation of the monocyte polarization or alteration of the cytokine expression pattern (Supplemental Fig. 3F).

Next, to restrict c-Jun deletion to macrophages and granulocytes, we induced arthritis in c-Jun$^{\Delta LysM}$ and littermate controls. Following induction of arthritis, *c-Jun* mRNA level was quantified in the joints of wild-type and mutant mice paws. Only ~25% decreased *c-Jun* mRNA levels could be detected in c-Jun$^{\Delta LysM}$ arthritic mice when compared with arthritic littermates, probably due to the expression of *c-Jun* by other cells present in the mice paws (Fig. 3A). However, similar to c-Jun$^{\Delta Mx}$ mice, c-Jun$^{\Delta LysM}$ mice showed less severe arthritis compared with littermate controls (Fig. 3B, 3C). In vivo MRI analysis confirmed reduced inflammation in c-Jun$^{\Delta LysM}$ mice, as shown by smaller paw volume and less contrast enhancement in the paws (Fig. 3D). Consistent with less severe arthritis, c-Jun$^{\Delta LysM}$ mice also showed a reduction of histological features of inflammation, bone erosion, and osteoclast accumulation when compared with wild-type controls (Fig. 3E). Taken together, these data revealed that c-Jun deletion in the myeloid lineage alleviates arthritic inflammation.

No altered macrophage numbers in the joints of c-Jun mutant mice

To investigate whether macrophage numbers were altered in arthritic c-Jun$^{\Delta Mx}$ and c-Jun$^{\Delta LysM}$ mice, flow cytometry analysis of the joints and the secondary lymphatic organs was performed. No differences in the percentages or absolute number of F4/80$^+$ cells or MHC class II$^+$ macrophages could be detected in bone marrow, spleen, blood, and ankle joints of respective wild-type controls and c-Jun$^{\Delta Mx}$ or c-Jun$^{\Delta LysM}$ mice (Fig. 3F, Supplemental Fig. 3G, Table I, and data not shown). Also, the numbers of Ly-6C$^+$ monocytes and Ly-6G$^+$ granulocytes were not altered in the joints of mutant and wild-type controls (data not shown). Apart from macrophages, we could not detect any differences in the distribution of T cell subsets in the arthritic joints, inguinal lymph nodes, blood, or the spleen between c-Jun$^{\Delta LysM}$ mice and wild-type controls (data not shown). Collectively, these data suggest that c-Jun influences arthritis by affecting macrophage signaling and proinflammatory mediator production rather than macrophage polarization or migration into inflammatory ankles.

c-Jun induces Cox2 but inhibits Arg1 expression in macrophages

To identify the molecular mechanism by which deficiency of c-Jun in macrophages mitigates arthritis, expression of target genes identified in the microarray was assessed in the joints of mutant and wild-type mice. Although subtle differences in expression patterns were found between c-Jun$^{\Delta Mx}$ and c-Jun$^{\Delta LysM}$ mice, several changes in pro- and anti-inflammatory factors were consistent among the two mutant strains. Reduced inflammation of paws in the c-Jun$^{\Delta LysM}$ mice was associated with increased mRNA levels of anti-inflammatory markers *Il10* and *Ym1*, as well as with decreased proinflammatory markers, such as *Il12b*, and signaling molecules, such as *Irf4*, *Klf4*, and *Socs2* (Fig. 4). Similarly, we also found upregulation of *Ym1* and a downregulation of *Klf4* and *Socs2* in the joints of c-Jun$^{\Delta Mx}$ mice as observed in the c-Jun$^{\Delta LysM}$ mutants (Supplemental Fig. 4A–C). In accordance with the in vitro findings, *Cox2* mRNA level was significantly decreased in the ankles of c-Jun$^{\Delta Mx}$ mice (Supplemental Fig. 4D). In c-Jun$^{\Delta LysM}$ mice, we did not find a significant decrease of *Cox2* mRNA, but quantification of Cox2 protein level by intracellular flow cytometry in macrophages isolated from arthritic ankles showed decreased Cox2 protein levels in c-Jun$^{\Delta LysM}$ mice (Fig. 5A, 5B).

c-Jun transcriptionally regulates Cox2 expression

Next, we determined whether c-Jun can transcriptionally regulate *Cox2* expression in macrophages. Bioinformatic promoter analysis revealed several AP-1 binding sites 3 kbp upstream of the *Cox2* gene. Indeed, ChIP analysis revealed that c-Jun can bind to the promoter ~1000 bp upstream of the *Cox2* starting site (Fig. 5C). Additionally, ChIP analysis for other AP-1 members revealed that c-Jun binds preferentially with the FOS member Fra-2 on the *Cox2* promoter site (Fig. 5D). Moreover, decreased Cox2 levels in the joints of c-Jun$^{\Delta LysM}$ and c-Jun$^{\Delta Mx}$ mice were associated with decreased expression of the Cox2 downstream gene *Ido1* (22, 23) (Fig. 5E, Supplemental Fig. 4E). Additionally, the level of PGE_2, which is produced by Cox2, was also reduced in the paws of c-Jun$^{\Delta LysM}$ mice when compared with wild-type controls (Fig. 5F). These data suggest that c-Jun, together with Fra-2, induces *Cox2* expression in macrophages and increases proinflammatory PGE_2 levels at the site of inflammation.

In addition to the induction of *Cox2*, c-Jun appears to repress *Arg1*. In vivo, *Arg1* was increased at mRNA levels in c-Jun$^{\Delta LysM}$ and c-Jun$^{\Delta Mx}$ ankles (Fig. 5G, Supplemental Fig. 4F). The increased expression of *Arg1* led to a tendency of higher arginase activity in ankle lysates from the mutant mice (Fig. 5H). The direct binding of c-Jun to the Arg1 promoter was investigated using ChIP analysis. However, unlike to the promoter of *Cox2*, c-Jun does not directly bind to the *Arg1* promoter (Fig. 5I). The specific binding of the Abs used for ChIP analysis was verified using c-Jun–deficient macrophages (Fig. 5C, 5D, 5I). These data demonstrate that c-Jun indirectly abrogates *Arg1* expression, which may also contribute to the proinflammatory effects of c-Jun.

Taken together, these results demonstrate that c-Jun is involved in proinflammatory macrophage activation. In particular, c-Jun transcriptionally regulates *Cox2* and indirectly inhibits *Arg1*. Consequently, the expression of c-Jun in macrophages promotes arthritic inflammation and bone erosion in the serum-induced arthritis model (Fig. 5J).

Discussion

AP-1 transcription factors have been involved in the regulation of inflammatory processes such as TLR4-mediated activation of macrophages by LPS. Indeed, AP-1 activation can act synergistically with NF-κB, resulting in the regulation of proinflammatory

thioglycollate-elicited macrophages from c-Jun$^{\Delta LysM}$ or control mice. The method of ChIP analysis is described above. Data are shown as means, and the error bars represent SEM from three independent experiments. *$p < 0.05$, **$p < 0.01$, ***$p < 0.001$ by Student *t* test (A, E and G) or ANOVA (B–D, F, H and I). (**J**) Scheme of c-Jun mechanism in macrophages: c-Jun regulates macrophage signaling through direct activation of *Cox2* and indirect inhibition of *Arg1*, which subsequently increases arthritis.

cytokines or chemokines (5, 24). In this study, we described a novel pathway of AP-1 regulating macrophage activation. We found that c-Jun is not only increased after LPS activation of macrophages, but it senses a wide range of macrophage activation signals, including Th1 and Th2 cytokines and pro- and anti-inflammatory stimuli, but also microbial products. Microarray expression data followed by GO and KEGG cluster analyses of c-Jun–deficient macrophages underscored the central role of c-Jun in regulating the expression of a wide range of cytokines produced by macrophages.

The functional role of c-Jun in regulating cytokine responses and inflammatory disease was supported by our data using two different conditional c-Jun–deficient mouse models (c-Jun$^{\Delta LysM}$ and c-Jun$^{\Delta Mx}$), which lack c-Jun in macrophages. Whereas the c-Jun$^{\Delta Mx}$ line shows a wider deletion in the hematopoietic lineage (13), c-Jun$^{\Delta LysM}$ mice show a more specific deletion in the monocytic lineage (14). Although c-Jun was still detectable at mRNA and protein levels in joints of c-Jun$^{\Delta LysM}$ and c-Jun$^{\Delta Mx}$ mice, upon the induction of arthritis inflammatory responses, the structural damages were mitigated in both c-Jun mutant lines with remarkably similar results. These findings extend previous findings by Fahmy et al. (25) who showed that global knockdown of c-Jun mitigated collagen Ab-induced arthritis.

c-Jun appears to represent a key transcriptional checkpoint in macrophages regulating the expression of several proinflammatory mediators. For instance, ChIP and in vitro gene profiling of stimulated mutant and wild-type macrophages showed that Cox2 in macrophages is directly controlled by c-Jun. Cox2 is responsible for elevated PGE_2 production (26, 27), which causes bone resorption and stimulates the release of matrix metalloproteinases that degrade cartilage (28). Cox2 inhibitors are widely used anti-inflammatory drugs in patients with arthritis, as they competitively inhibit Cox2 and block PG production at sites of inflammation (29, 30). In accordance with human data obtained in rheumatoid arthritis patients (31, 32), we also showed that Cox2 protein level is increased in articular macrophages from arthritic mice. Furthermore, our study showed a decrease of Cox2 activity in c-Jun–deficient mice correlating with reduced PGE_2 protein level in the joint of mutant mice. The PGE_2 production by Cox2 was not completely abrogated, which might be due to other regulators of *Cox2* expression (33, 34) and *Cox2* expression by other cells in the synovium, such as osteoblasts and synovial fibroblasts (35, 36). An additional interesting observation from the c-Jun regulatory network analysis was that Cox2 was located in the response-to-hypoxia cluster, which attributes to the fact that Cox2 stabilizes Hif-1α and that the articular tissue is hypoxic in arthritis (37, 38).

Another pathway by which c-Jun regulates the severity of inflammation is the Arg1 pathway that we found increased in the c-Jun–deleted macrophages. Arg1 is an enzyme that hydrolyzes arginine to urea and ornithine. The expression of Arg1 in the myeloid lineage is predominantly regulated by exogenous stimuli in a STAT3- or STAT6-dependent manner and is commonly thought to characterize alternatively activated macrophages involved in resolution of inflammation and tissue repair (39–42). Only recently, it was shown that alternatively activated macrophages expressing *Arg1* contribute to resolve the inflammation of inflammatory arthritis (43). c-Jun downregulates *Arg1* possibly by involving other AP-1 members and thereby counteracts the resolution of inflammation. The factors acting downstream of c-Jun abrogating *Arg1* expression need to be further investigated.

In summary, we show that c-Jun regulates a program of pro- and anti-inflammatory gene expression during macrophage activation and thereby influences the severity of arthritis. First, the direct regulation of Cox2 by c-Jun increases PGE_2 levels and sustains arthritis. Second, c-Jun inhibits *Arg1* expression, which blocks resolution of arthritis and negatively regulate tissue repair. Taken together, our results show that c-Jun acts as a checkpoint during macrophage activation, shifting their responses toward a proinflammatory phenotype. Hence, c-Jun may represent an interesting therapeutic target in rheumatoid arthritis.

Acknowledgments

We thank Dr. Wolfgang Baum for assistance with animal experiments and preparation of the K/BxN serum, and Christine Zech, Barbara Happich, and Hedwig Symowski for great technical assistance. We kindly thank Daniel Eriksson for critically reading the manuscript.

Disclosures

The authors have no financial conflicts of interest.

References

1. Zenz, R., R. Eferl, C. Scheinecker, K. Redlich, J. Smolen, H. B. Schonthaler, L. Kenner, E. Tschachler, and E. F. Wagner. 2008. Activator protein 1 (Fos/Jun) functions in inflammatory bone and skin disease. *Arthritis Res. Ther.* 10: 201.
2. Okamoto, H., T. P. Cujec, H. Yamanaka, and N. Kamatani. 2008. Molecular aspects of rheumatoid arthritis: role of transcription factors. *FEBS J.* 275: 4463–4470.
3. Hagemann, T., S. K. Biswas, T. Lawrence, A. Sica, and C. E. Lewis. 2009. Regulation of macrophage function in tumors: the multifaceted role of NF-κB. *Blood* 113: 3139–3146.
4. Xue, J., S. V. Schmidt, J. Sander, A. Draffehn, W. Krebs, I. Quester, D. De Nardo, T. D. Gohel, M. Emde, L. Schmidleithner, et al. 2014. Transcriptome-based network analysis reveals a spectrum model of human macrophage activation. *Immunity* 40: 274–288.
5. Guha, M., and N. Mackman. 2001. LPS induction of gene expression in human monocytes. *Cell. Signal.* 13: 85–94.
6. Behmoaras, J., G. Bhangal, J. Smith, K. McDonald, B. Mutch, P. C. Lai, J. Domin, L. Game, A. Salama, B. M. Foxwell, et al. 2008. *Jund* is a determinant of macrophage activation and is associated with glomerulonephritis susceptibility. *Nat. Genet.* 40: 553–559.
7. Srivastava, P. K., R. P. Hull, J. Behmoaras, E. Petretto, and T. J. Aitman. 2013. JunD/AP1 regulatory network analysis during macrophage activation in a rat model of crescentic glomerulonephritis. *BMC Syst. Biol.* 7: 93.
8. Han, M. S., D. Y. Jung, C. Morel, S. A. Lakhani, J. K. Kim, R. A. Flavell, and R. J. Davis. 2013. JNK expression by macrophages promotes obesity-induced insulin resistance and inflammation. *Science* 339: 218–222.
9. Han, Z., D. L. Boyle, L. Chang, B. Bennett, M. Karin, L. Yang, A. M. Manning, and G. S. Firestein. 2001. c-Jun N-terminal kinase is required for metalloproteinase expression and joint destruction in inflammatory arthritis. *J. Clin. Invest.* 108: 73–81.
10. Helmick, C. G., D. T. Felson, R. C. Lawrence, S. Gabriel, R. Hirsch, C. K. Kwoh, M. H. Liang, H. M. Kremers, M. D. Mayes, P. A. Merkel, et al; National Arthritis Data Workgroup. 2008. Estimates of the prevalence of arthritis and other rheumatic conditions in the United States. Part I. *Arthritis Rheum.* 58: 15–25.
11. Picerno, V., F. Ferro, A. Adinolfi, E. Valentini, C. Tani, and A. Alunno. 2015. One year in review: the pathogenesis of rheumatoid arthritis. *Clin. Exp. Rheumatol.* 33: 551–558.
12. Kinne, R. W., R. Bräuer, B. Stuhlmüller, E. Palombo-Kinne, and G. R. Burmester. 2000. Macrophages in rheumatoid arthritis. *Arthritis Res.* 2: 189–202.
13. Kühn, R., F. Schwenk, M. Aguet, and K. Rajewsky. 1995. Inducible gene targeting in mice. *Science* 269: 1427–1429.
14. Clausen, B. E., C. Burkhardt, W. Reith, R. Renkawitz, and I. Förster. 1999. Conditional gene targeting in macrophages and granulocytes using LysMcre mice. *Transgenic Res.* 8: 265–277.
15. Palmada, M., S. Kanwal, N. J. Rutkoski, C. Gustafson-Brown, R. S. Johnson, R. Wisdom, and B. D. Carter. 2002. *c-jun* is essential for sympathetic neuronal death induced by NGF withdrawal but not by p75 activation. [Published erratum appears in 2003 *J. Cell Biol.* 161: 439.] *J. Cell Biol.* 158: 453–461.
16. Carey, M. F., C. L. Peterson, and S. T. Smale. 2009. Chromatin immunoprecipitation (ChIP). *Cold Spring Harb. Protoc.* 2009: pdb prot5279. doi:10.1101/pdb.prot5279
17. Corraliza, I. M., M. L. Campo, G. Soler, and M. Modolell. 1994. Determination of arginase activity in macrophages: a micromethod. *J. Immunol. Methods* 174: 231–235.
18. Shannon, P., A. Markiel, O. Ozier, N. S. Baliga, J. T. Wang, D. Ramage, N. Amin, B. Schwikowski, and T. Ideker. 2003. Cytoscape: a software environment for integrated models of biomolecular interaction networks. *Genome Res.* 13: 2498–2504.
19. Bindea, G., B. Mlecnik, H. Hackl, P. Charoentong, M. Tosolini, A. Kirilovsky, W. H. Fridman, F. Pagès, Z. Trajanoski, and J. Galon. 2009. ClueGO: a Cytoscape plug-in to decipher functionally grouped gene ontology and pathway annotation networks. *Bioinformatics* 25: 1091–1093.

20. Monach, P. A., D. Mathis, and C. Benoist. 2008. The K/BxN arthritis model. *Curr. Protoc. Immunol.* Chapter 15: Unit 15.22. doi:10.1002/0471142735.im1522s81
21. Brand, D. D., K. A. Latham, and E. F. Rosloniec. 2007. Collagen-induced arthritis. *Nat. Protoc.* 2: 1269–1275.
22. Trabanelli, S., M. Lecciso, V. Salvestrini, M. Cavo, D. Očadlíková, R. M. Lemoli, and A. Curti. 2015. PGE_2-induced IDO1 inhibits the capacity of fully mature DCs to elicit an in vitro antileukemic immune response. *J. Immunol. Res.* 2015: 253191.
23. Iachininoto, M. G., E. R. Nuzzolo, G. Bonanno, A. Mariotti, A. Procoli, F. Locatelli, R. De Cristofaro, and S. Rutella. 2013. Cyclooxygenase-2 (COX-2) inhibition constrains indoleamine 2,3-dioxygenase 1 (IDO1) activity in acute myeloid leukaemia cells. *Molecules* 18: 10132–10145.
24. Kim, D. S., J. H. Han, and H. J. Kwon. 2003. NF-κB and c-Jun-dependent regulation of macrophage inflammatory protein-2 gene expression in response to lipopolysaccharide in RAW 264.7 cells. *Mol. Immunol.* 40: 633–643.
25. Fahmy, R. G., A. Waldman, G. Zhang, A. Mitchell, N. Tedla, H. Cai, C. R. Geczy, C. N. Chesterman, M. Perry, and L. M. Khachigian. 2006. Suppression of vascular permeability and inflammation by targeting of the transcription factor c-Jun. *Nat. Biotechnol.* 24: 856–863.
26. Claveau, D., M. Sirinyan, J. Guay, R. Gordon, C. C. Chan, Y. Bureau, D. Riendeau, and J. A. Mancini. 2003. Microsomal prostaglandin E synthase-1 is a major terminal synthase that is selectively up-regulated during cyclooxygenase-2-dependent prostaglandin E_2 production in the rat adjuvant-induced arthritis model. *J. Immunol.* 170: 4738–4744.
27. McCoy, J. M., J. R. Wicks, and L. P. Audoly. 2002. The role of prostaglandin E_2 receptors in the pathogenesis of rheumatoid arthritis. *J. Clin. Invest.* 110: 651–658.
28. Miyaura, C., M. Inada, T. Suzawa, Y. Sugimoto, F. Ushikubi, A. Ichikawa, S. Narumiya, and T. Suda. 2000. Impaired bone resorption to prostaglandin E_2 in prostaglandin E receptor EP4-knockout mice. *J. Biol. Chem.* 275: 19819–19823.
29. Cha, H. S., K. S. Ahn, C. H. Jeon, J. Kim, and E. M. Koh. 2004. Inhibitory effect of cyclo-oxygenase-2 inhibitor on the production of matrix metalloproteinases in rheumatoid fibroblast-like synoviocytes. *Rheumatol. Int.* 24: 207–211.
30. Crofford, L. J. 2013. Use of NSAIDs in treating patients with arthritis. *Arthritis Res. Ther.* 15(Suppl. 3): S2.
31. Martel-Pelletier, J., J. P. Pelletier, and H. Fahmi. 2003. Cyclooxygenase-2 and prostaglandins in articular tissues. *Semin. Arthritis Rheum.* 33: 155–167.
32. Sano, H., T. Hla, J. A. Maier, L. J. Crofford, J. P. Case, T. Maciag, and R. L. Wilder. 1992. In vivo cyclooxygenase expression in synovial tissues of patients with rheumatoid arthritis and osteoarthritis and rats with adjuvant and streptococcal cell wall arthritis. *J. Clin. Invest.* 89: 97–108.
33. Hellmann, J., Y. Tang, M. J. Zhang, T. Hai, A. Bhatnagar, S. Srivastava, and M. Spite. 2015. Atf3 negatively regulates Ptgs2/Cox2 expression during acute inflammation. *Prostaglandins Other Lipid Mediat.* 116–117: 49–56.
34. Tanabe, T., and N. Tohnai. 2002. Cyclooxygenase isozymes and their gene structures and expression. *Prostaglandins Other Lipid Mediat.* 68–69: 95–114.
35. Chikazu, D., X. Li, H. Kawaguchi, Y. Sakuma, O. S. Voznesensky, D. J. Adams, M. Xu, K. Hoshio, V. Katavic, H. R. Herschman, et al. 2002. Bone morphogenetic protein 2 induces cyclo-oxygenase 2 in osteoblasts via a Cbfal binding site: role in effects of bone morphogenetic protein 2 in vitro and in vivo. *J. Bone Miner. Res.* 17: 1430–1440.
36. Faour, W. H., Y. He, Q. W. He, M. de Ladurantaye, M. Quintero, A. Mancini, and J. A. Di Battista. 2001. Prostaglandin E_2 regulates the level and stability of cyclooxygenase-2 mRNA through activation of p38 mitogen-activated protein kinase in interleukin-1β-treated human synovial fibroblasts. *J. Biol. Chem.* 276: 31720–31731.
37. Biddlestone, J., D. Bandarra, and S. Rocha. 2015. The role of hypoxia in inflammatory disease (review). *Int. J. Mol. Med.* 35: 859–869.
38. Huang, S. P., M. S. Wu, C. T. Shun, H. P. Wang, C. Y. Hsieh, M. L. Kuo, and J. T. Lin. 2005. Cyclooxygenase-2 increases hypoxia-inducible factor-1 and vascular endothelial growth factor to promote angiogenesis in gastric carcinoma. *J. Biomed. Sci.* 12: 229–241.
39. Campbell, L., C. R. Saville, P. J. Murray, S. M. Cruickshank, and M. J. Hardman. 2013. Local arginase 1 activity is required for cutaneous wound healing. *J. Invest. Dermatol.* 133: 2461–2470.
40. Biswas, A., A. Bhattacharya, S. Kar, and P. K. Das. 2011. Expression of IL-10-triggered STAT3-dependent IL-4Rα is required for induction of arginase 1 in visceral leishmaniasis. *Eur. J. Immunol.* 41: 992–1003.
41. Pesce, J. T., T. R. Ramalingam, M. M. Mentink-Kane, M. S. Wilson, K. C. El Kasmi, A. M. Smith, R. W. Thompson, A. W. Cheever, P. J. Murray, and T. A. Wynn. 2009. Arginase-1-expressing macrophages suppress Th2 cytokine-driven inflammation and fibrosis. *PLoS Pathog.* 5: e1000371.
42. Morris, S. M., Jr. 2007. Arginine metabolism: boundaries of our knowledge. *J. Nutr.* 137(6, Suppl. 2): 1602S–1609S.
43. Chen, Z., D. Andreev, K. Oeser, B. Krljanac, A. Hueber, A. Kleyer, D. Voehringer, G. Schett, and A. Bozec. 2016. Th2 and eosinophil responses suppress inflammatory arthritis. *Nat. Commun.* 7: 11596.